Experimental study of the response of semiconductor detectors to low-energy photons

M.C. Lépy[a],[*], J.L. Campbell[b], J.M. Laborie[a], J. Plagnard[a], P. Stemmler[c], W.J. Teesdale[b]

[a]*CEA/DAMRI, BNM/Laboratoire Primaire des Rayonnements Ionisants, BP 52 F-91193 Gif-sur-Yvette Cedex, France*
[b]*University of Guelph, Guelph, Ont., N1G 2W1, Canada*
[c]*CEA/DAM, DRIF/DCRE/Service Diagnostics Expérimentaux, BP 52 F-91680 Bruyères-le-Châtel, France*

Abstract

Six semiconductor detectors (Si(Li) and HPGe) are calibrated in the 1–10 keV energy range by means of tuneable monochromatised synchrotron radiation. Significant improvement in the quality of the response is observed in very recent detectors. A peak shape calibration is established using a modified Hypermet-type function to model the detector response for each energy step; electron effects induce individual background and tail shapes for each detector material. Fano factors for both semiconductor materials are experimentally derived. The efficiency calibration is determined using a proportional counter as reference: the front semiconductor layer acts as a partially active zone. © 2000 Elsevier Science B.V. All rights reserved.

1. Introduction

Significant improvement has been noticed in the quality response of very recent semiconductor photon detectors used in the low-energy range [1]. In parallel, new features such as the radiative Auger effect and satellite lines are distinguished in complex X-ray spectra [1]. Both facts should improve the detailed analysis of electronic shells rearrangement spectra and the relevant accuracy of analysis methods based on X-ray emission (XRF, PIXE, etc.). However, complementary experiments are still needed to provide further details about the response characteristics of the detectors. A number of experimental studies concerning the response of silicon detectors in the 1–10 keV energy range have been published in the last few years [1–3]. But, as they have not yet been used in this energy range no such information is available for the germanium detectors. It has been shown that tuneable monochromatized synchrotron radiation is a very convenient tool for examining the response of a photon detector versus the incident energy [2]. This characterisation must include the efficiency and the peak shape calibration as both depend on the incident energy. It is thus worth using this source to compare performances of silicon and germanium detectors, focusing on some characteristics of the latter as their response has been less studied in the low-energy range.

*Corresponding author. Tel.: + 33-1-69-08-4775; fax: + 33-1-69-08-9529.

E-mail address: marie-christine.lepy@cea.fr (M.C. Lépy)

2. Experimental arrangement

2.1. Calibration set-up

Measurements are carried out at the beam line SB3 of the storage ring Super ACO, at the Laboratoire pour l'Utilisation du Rayonnement Electromagnétique (LURE), in Orsay, France. The calibration station, equipped by the Service Diagnostics Expérimentaux (CEA), includes a double-crystal monochromator which selects a mono-energetic radiation in the continuous synchrotron beam [2]. The semiconductor detector (SD) to be characterised is set at the end of the beam line, and the selected radiation impinges on the SD window connected to the vacuum of the calibration chamber. A reference proportional counter (PC) can be interposed in the monochromatic radiation path to measure the incident beam intensity. Two kinds of characterisation can then be performed. First, the efficiency calibration is obtained by comparing, for the same monoenergetic radiation, the count rates on the SD and on the PC, whose efficiency is easily computed. This comparative method is also used to study the discontinuities at the absorption edges of the detector. Second, the study of the spectrum shape versus energy allows characterisation of the response of the SD to a monochromatic line. This shape calibration is mainly of interest for processing complex X-ray spectra.

2.2. Detectors characteristics

Up to now, the silicon detectors have been preferably employed in the soft X-ray energy region. However, as a result of manufacturing technology improvements, dead layers of germanium detectors are becoming thinner thus allowing these devices to detect lower energies. Six different detectors with two kinds of semiconductor material (lithium-drifted silicon (Si(Li)) and high-purity germanium (HPGe)) are then studied using the above calibration arrangement. They are all equipped with an entrance window: these are traditional beryllium or special "low-energy" windows consisting of a light element polymer on a grid. Some simple characteristics are measured using 6 keV monochromatic radiation and are given in Table 1: the individual characteristics provide information about the ability of the SD to separate two close lines and to detect low-intensity peaks. The resolution (FWHM) of the main peak is determined by fitting its shape by a Gaussian function. It is generally accepted that the peak width includes two main contributions: a constant part mainly due to electronic noise and an energy-dependent component resulting from the statistical scattering of the number of charge carriers created in the bulk of the semiconductor. The statistical variation of the number of electron–hole pairs depends on the incident energy, E, on the Fano factor of the semiconductor material, F, and on the mean pair creation

Table 1
Characteristics of the studied detectors

Detector number	Si(Li) 1	Si(Li) 2	Si(Li) 3	Si(Li) 4	HPGe 5	HPGe 6
Active area (mm^2)	30	30	12	12	10	20
Thickness (mm)	5	3	3	3	2.5	5
Window material	Beryllium	Beryllium	Beryllium	Beryllium	Composite	Composite on an Si grid
Window thickness (μm)	10	25	7.5	10		
Contact	Au	Not given	Au — 20 nm	Au	Not given	Not given
Assumed dead layer	No		Si — 0.2 μm	No		
FWHM at 6 keV	161 eV	138 eV	140 eV	170 eV	113 eV	147 eV
σ_0^2	2250 (15)	911 (56)	748 (6)	2671 (10)	530 (7)	2085 (16)
Fw	0.4070 (48)	0.4240 (108)	0.4571 (52)	0.4236 (25)	0.2953 (16)	0.3208 (23)
Peak-to-background (6 keV)	1870	25 800	2500	3650	15 900	8200
FWHM with ^{55}Fe (eV)	165	140	Not measured	171	115	148
Peak-to-background (^{55}Fe)	680	14 080	Not measured	2970	10 800	3540
Peak-to-valley (^{55}Fe)	330	490	Not measured	280	620	390

energy, w. The standard deviation of the Gaussian representing the main part of the relevant peak, can then be expressed as a function of the energy, E:

$$\sigma^2(E) = \sigma_0^2 + FwE.$$

Thus, for each studied SD, the linear fitting of σ^2 versus the energy allows deriving the value of Fw. Assuming no significant variation of Fw in the 1–10 keV energy range, Table 1 shows the coefficients values obtained using the present experimental arrangement, with the combined standard uncertainties in parenthesis. The peak-to-background ratio is the ratio of the intensity of the peak to the mean intensity measured in the 900–1100 eV
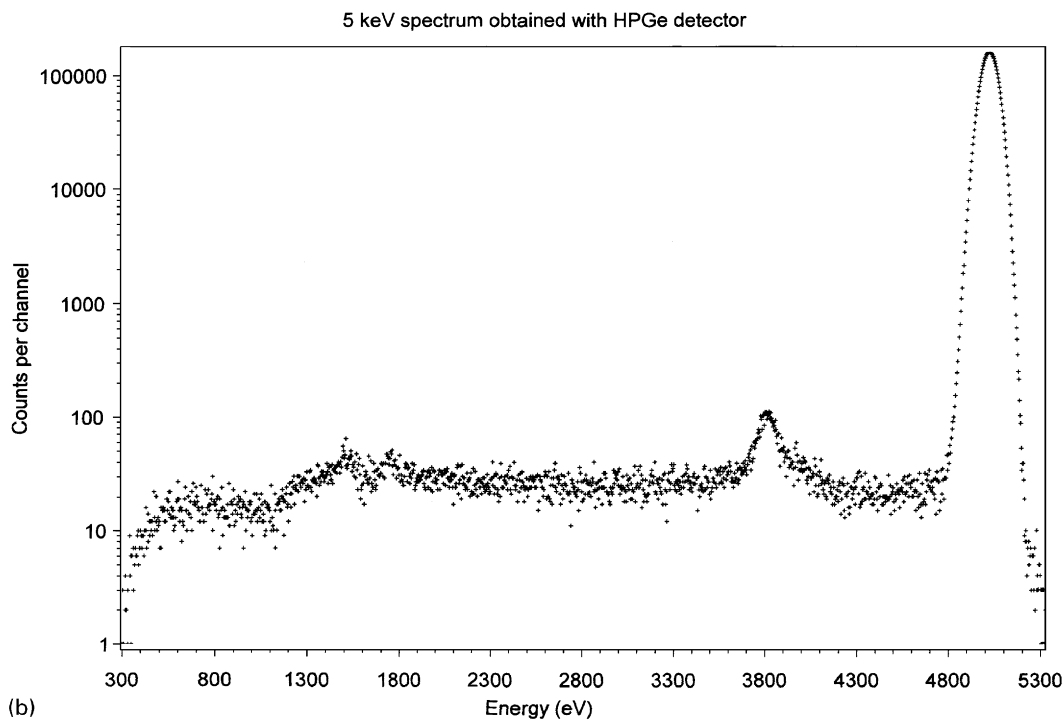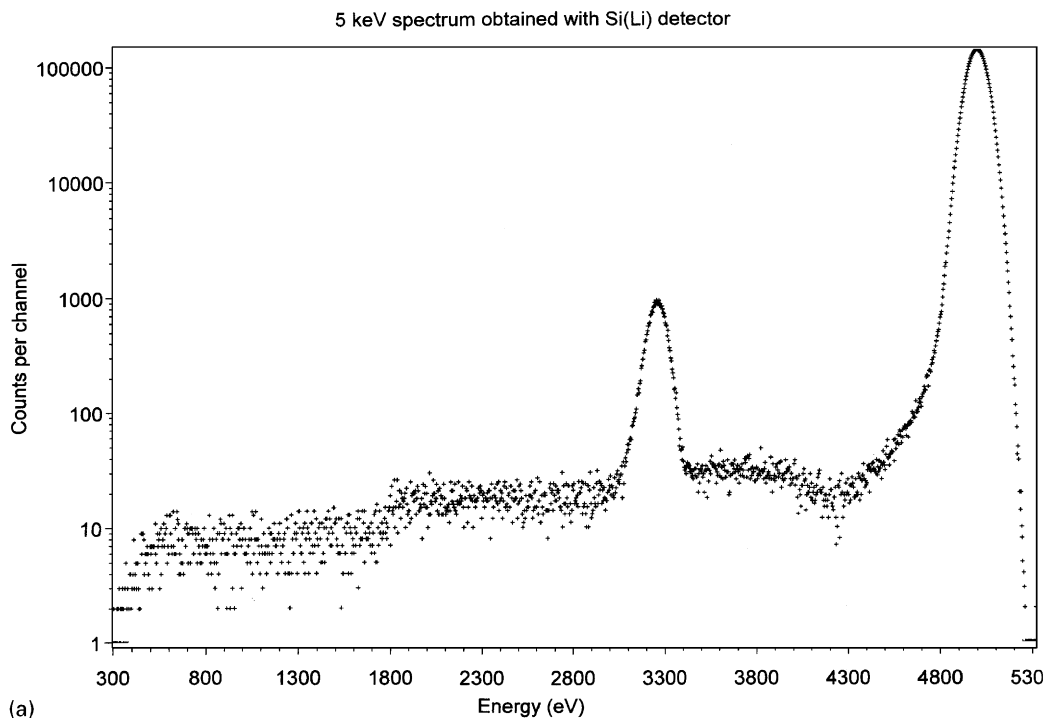
Fig. 1. (a) Spectrum obtained with 5 keV monochromatic photons for Si(Li) detector 2. (b) Spectrum obtained with 5 keV monochromatic photons for HPGe detector 5.
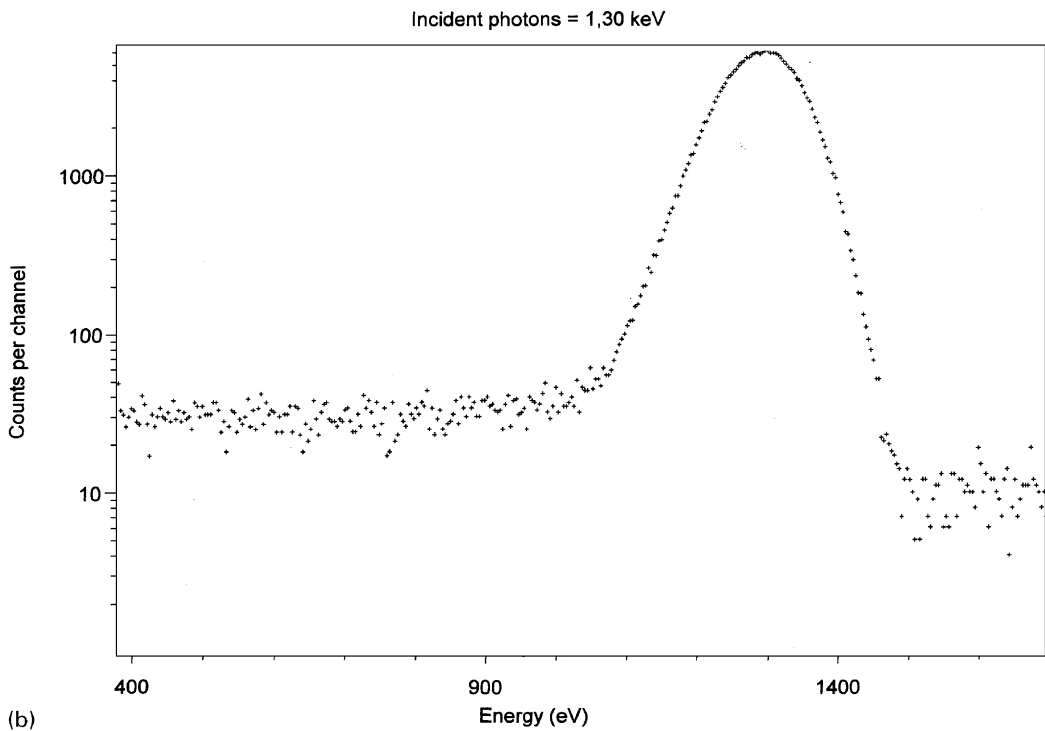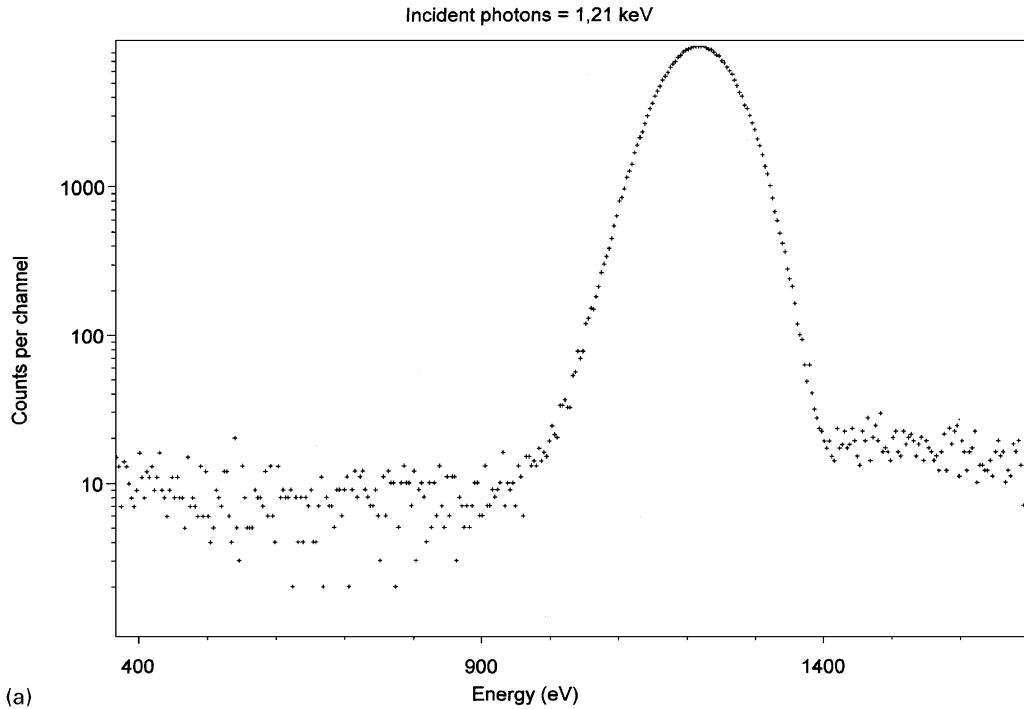
Fig. 2. (a) Spectrum obtained with HPGe detector 6 with 1.21 keV incident photons (below germanium L3 binding energy). (b) Spectrum obtained with HPGe detector 6 with 1.30 keV incident photons (after germanium L2 binding energy).

remaining pertinent: only the continuous part of the tail, $S(E)$ has not exactly the right shape, nevertheless its mean amplitude gives useful information. It must be noted that the truncated step, $ST(E)$ need not be included for germanium detectors nor for higher energies in the case of silicon detectors. The peak shape calibration and the relevant parameters such as peak position, width and area, can then be used to derive complementary information about the SD response, respectively the pair creation energy, the Fano factor and the efficiency.

4. Pair creation energy and Fano factor

4.1. Pair creation energy

The pulse intensity recorded at the SD electrode is proportional to the number of charge carriers created by the photon interaction. There is currently an open discussion about the mean energy required for creating an electron–hole pair, w, in the soft energy range and its variation around the binding energies and versus the temperature. For silicon, energy dependence is shown for energies below some hundreds of eV [7], and different studies lead to discrepant conclusions about a variation around the K binding energy [8,9]. As the analog-to-digital conversion process is linear, the resulting position of the peak would provide information on the mean

number of charges created in the detector. Fig. 3 presents the recorded peak position versus the incident energy for Si(Li) detector 3. If the position value is normalised at the pair creation energy for the high energy, taken as 3.81 eV at 2.5 keV, one can derive the w value around the K silicon binding energy. In fact, there is a marked discontinuity and the relevant w value shows a step from about 3.808 to 3.816 eV, which represents a 0.2% increase, slightly lower than given in Ref. [8]. However, as was pointed out earlier, the shape of the peak changes significantly above the binding energy: the linear attenuation coefficient undergoes sudden and large variations as an effect of the extended X-ray absorption fine structure (EXAFS); moreover the peak position results from the mathematical fitting and its associated uncertainty increases as the peak shape deviates from a Gaussian shape. Both facts prevent deriving any further conclusion from the present experiment.

4.2. Fano factor

The Fw mean values, derived from the square Gaussian standard deviation linear fitting (Table 1), are respectively 0.426 (15) and 0.304 (12) for silicon and germanium. The present silicon mean value is consistent with previously published data [8,11,13], however, for germanium [11–13], it appears rather low. But, as different kinds of detectors
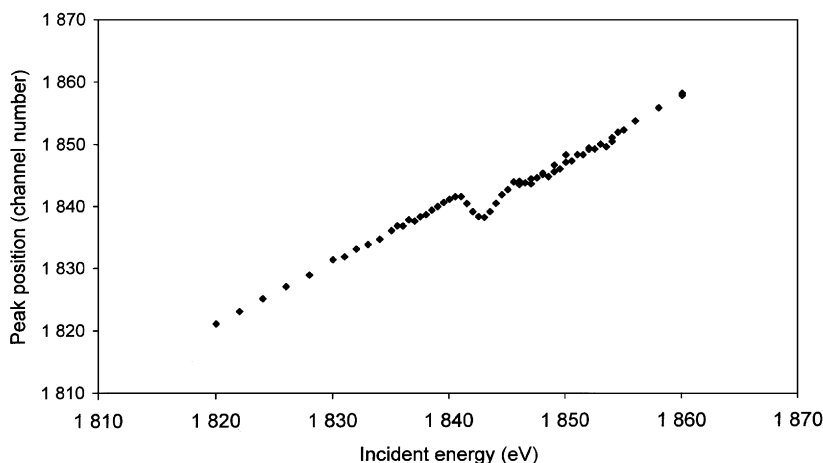

Fig. 3. Fitted peak position versus incident energy for Si(Li) detector 3.

(CCD, Si(Li), etc.) are compared at different temperatures and for different incident energies, it is difficult to draw any conclusion from the scarce published data. With the hypothesis of a constant pair creation energy of 3.81 eV for silicon and 2.97 eV for germanium (at the detector working temperature of 77 K), the derived Fano factors, are respectively between 0.106 (detector 1) and 0.120 (detector 3), and 0.099 (detector 5) and 0.108 (detector 6).

5. Efficiency calibration

For each incident energy E, the detector efficiency $\varepsilon(E,\mathrm{SD})$ is computed as the ratio of the counts rates recorded on the detector and on the reference PC, respectively $N(E,\mathrm{SD})$ and $N(E,\mathrm{PC})$, taking account of the PC efficiency, $\varepsilon(E,\mathrm{PC})$:

$$\varepsilon(E,\mathrm{SD}) = \frac{N(E,\mathrm{SD})}{N(E,\mathrm{PC})}\,\varepsilon(E,\mathrm{PC}).$$

For Si(Li) detectors, it has been shown that two efficiencies can be distinguished, depending on the peak definition and consequently its area determination [2]: if only the Gaussian part of the peak is considered, the full-energy peak efficiency is defined; if the peak area includes the tailing and escape peak, the relevant value is known as the total efficiency. Fig. 4 shows the relevant efficiencies computed for HPGe detector 6: in both curves, a discontinuity absorption due to the presence of aluminium in the entrance window appears clearly (Al K binding energy = 1.56 keV). However, around the germanium L binding energies, in the 1.22–1.41 keV range, the dramatic decrease in the full-energy peak efficiency is nearly inexistent for the total efficiency. This means that, for the detector under study, the germanium front layer is not strictly dead, thus acting just as an absorber of the photon beam, but is a partially active zone leading only to incomplete charge collection.

6. Conclusion

This summary of the characteristics of some low-energy SDs points out the wide range of response quality that can be achieved in the current experimental set-ups. These results have to be weighted by the detector size, as the efficiency can be a major parameter, depending on the objective of the experiment. Moreover, the technology is still evolving and the presented characteristics are expected to be improved in the near future. As stated above, the classical mathematical model appears insufficient to accurately describe spectra obtained with the most recent detectors: a more sophisticated mathematical description would require
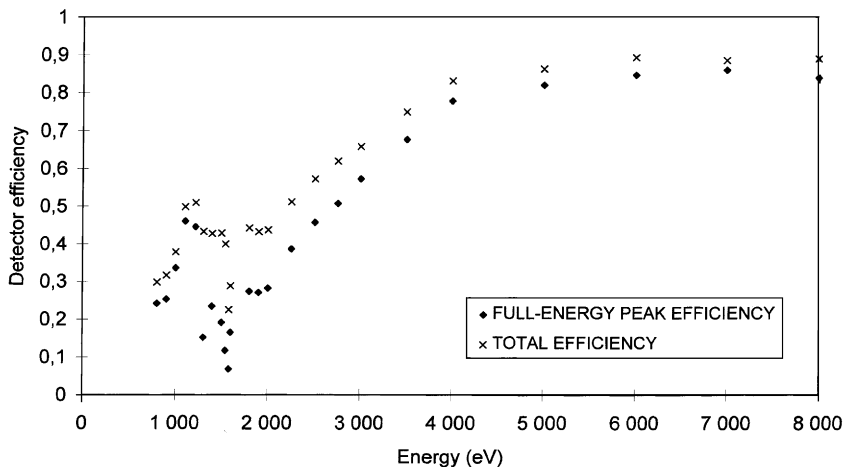

Fig. 4. Efficiency calibration for HPGe detector 6.

including the shapes due to weak physical effects such as escape electron humps. Monte Carlo simulations will help to accurately describe these phenomena [4], leading to a better understanding of the secondary electrons interaction in the different parts of the detectors. To our knowledge, this study is one of the first characterisations of germanium detectors in the soft X-ray range and their capability is clearly demonstrated; however, as their use in the low-energy region is new, complementary experimental studies need to be undertaken to obtain their detailed response with special attention to the vicinity of the germanium K and L binding energies. This information will be of major interest in the study of complex X-ray spectra, taking account of secondary phenomena such as radiative Auger effect and satellite lines [1,10]. Germanium detectors could be further used in X-ray emission analysis systems and their automated software suites, to take advantage of their superior resolution and excellent overall response.

References

[1] J.L. Campbell, J.A. Maxwell, T. Papp, G. White, X-Ray Spectrom. 26 (1997) 223.

[2] M.C. Lépy, J. Plagnard, P. Stemmler, G. Ban, L. Beck, P. Dhez, X-Ray Spectrom. 26 (1977) 195.

[3] F. Schloze, G. Ulm, Nucl. Instr. and Meth. A 339 (1994) 49.

[4] J.L. Campbell, G. Cauchon, M.C. Lépy, L. McDonald, J. Plagnard, P. Stemmler, W.J. Teesdale, G. White, Nucl. Instr. and Meth. A 418 (1998) 394.

[5] G.W. Philips, K.M. Marlow, Nucl. Instr. and Meth. 137 (1976) 525.

[6] H. Ruellan, M.C. Lépy, M. Etcheverry, J. Plagnard, J. Morel, Nucl. Instr. and Meth. A 369 (1996) 651.

[7] P. Lechner, R. Hartmann, H. Soltau, L. Strüder, Nucl. Instr. and Meth. A 377 (1996) 206.

[8] A. Owens, G.W. Fraser, A.F. Abbey, A. Holland, K. McCarthy, A. Keay, A. Wells, Nucl. Instr. and Meth. A 382 (1996) 503.

[9] F. Scholze, H. Rabus, G. Ulm, Appl. Phys. Lett. 69 (20) (1996) 2974.

[10] M.C. Lépy, M.M. Bé, J. Plagnard, AIP Conf. Proc. 392 (1997) 1067.

[11] R. Casanova Alig, Phys. Rev. B 27 (2) (1983) 968.

[12] S. Croft, D.S. Bond, Appl. Radiat. Isot. 42 (11) (1991) 1009.

[13] B.G. Lowe, Nucl. Instr. and Meth. A 399 (1997) 354.